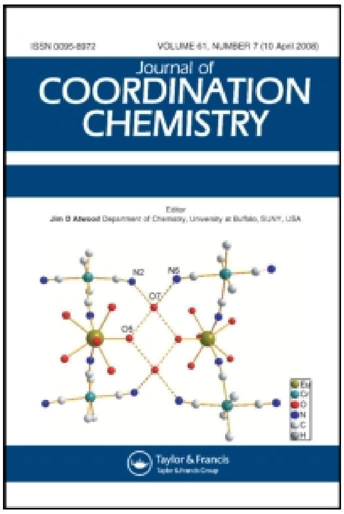

Journal of Coordination Chemistry

Publication details, including instructions for authors and subscription information:
http://www.informaworld.com/smpp/title~content=t713455674

Two spin systems based on [Ni(dmit)$_2$]$^-$ building blocks exhibiting 1-D chain and 2-D sheet structures: crystal structures and magnetic properties

Hai-Bao Duan[a]; Fang Xuan[a]; Xiao-Ming Ren[a]; Zheng-Fang Tian[a]; Lin-Jiang Shen[a]
[a] College of Science, Nanjing University of Technology, Nanjing 210009, P.R. China

To cite this Article Duan, Hai-Bao , Xuan, Fang , Ren, Xiao-Ming , Tian, Zheng-Fang and Shen, Lin-Jiang(2009) 'Two spin systems based on [Ni(dmit)$_2$]$^-$ building blocks exhibiting 1-D chain and 2-D sheet structures: crystal structures and magnetic properties', Journal of Coordination Chemistry, 62: 23, 3772 — 3781

To link to this Article: DOI: 10.1080/00958970903159149

URL: http://dx.doi.org/10.1080/00958970903159149

Journal of Coordination Chemistry
Vol. 62, No. 23, 10 December 2009, 3772–3781

Taylor & Francis
Taylor & Francis Group

Two spin systems based on $[Ni(dmit)_2]^-$ building blocks exhibiting 1-D chain and 2-D sheet structures: crystal structures and magnetic properties

HAI-BAO DUAN, FANG XUAN, XIAO-MING REN*,
ZHENG-FANG TIAN and LIN-JIANG SHEN*

College of Science, Nanjing University of Technology, Nanjing 210009, P.R. China

(*Received 17 April 2009; in final form 12 May 2009*)

The crystal structures and magnetic properties for two ion-pair complexes, $[MG][Ni(dmit)_2]$ (**1**) and $[RhB][Ni(dmit)_2]$ (**2**) (MG^+ = N-(4-((4-(dimethylamino)phenyl)(phenyl)methylene)cyclohexa-2,5-dienylidene)-N-methylmethanaminium, RhB^+ = 9-(2-carboxyphenyl)-3,6-bis(diethylamino)xanthylium; $dmit^{2-}$ = 1,3-dithiole-2-thione-4,5-dithiolate), have been investigated. Complex **1** crystallizes in the monoclinic space group $P2_1/c$, the stacking interactions between the GM^+ and $[Ni(dmit)_2]^-$ lead to the anion exhibiting a banana-shaped molecular geometry; the neighboring anions form a 1-D alternating chain along the crystallographic [1 1 0] direction via intermolecular lateral-to-lateral and head-to-head $S\cdots S$ contacts. The temperature dependence of magnetic susceptibility from 2–350 K does not display the magnetic character of a 1-D chain; the magnetic susceptibility data were fit to the Curie–Weiss equation to give $C = 0.351(15)\ \text{emu K mol}^{-1}$, $\theta = -3.51(28)$ K, and $\chi_0 = 8.00(3) \times 10^{-5}\ \text{emu mol}^{-1}$. Complex **2** belongs to the triclinic space group *P*-1 with two crystallographic inequivalent $[Ni(dmit)_2]^-$ anions, which exhibit perfect planar geometry. Two ethyl groups of RhB^+ are disordered over two positions at 296 K, and one becomes ordered at 150 K. The $[Ni(dmit)_2]^-$ anions form a 2-D molecular layer via intermolecular lateral-to-lateral and head-to-lateral $S\cdots S$ interactions with the anionic layer parallel to the crystallographic (0 1 −1) plane. The temperature variation of magnetic susceptibility from 2 to 350 K shows that antiferromagnetic coupling dominates in the anionic layer, and the disorder–order changes of cationic structure are not coupled to magnetic property.

Keywords: Bis(1,3-dithiole-2-thione-4,5-dithiolate)nickelate monoanion; Crystal structure; Magnetic property

1. Introduction

The use of bis(dithiolato)metalate complexes as building units in the construction of molecule based materials has received extensive attention due to their potential applications in near-infrared dyes [1, 2], conducting [3, 4], ferroelectric [5], magnetic [6, 7], or nonlinear optical materials [8, 9]. The planar $[M(mnt)_2]^-$ anions (mnt^{2-} = maleonitriledithiolate; M = Ni, Pt or Pt) with S = ½ spin form face-to-face stacks via intermolecular $M\cdots M$, $M\cdots S$, $S\cdots S$, and $\pi\cdots\pi$ interactions, giving

---

*Corresponding authors. Email: xmren@njut.edu.cn; ljshen@njust.edu.cn

Journal of Coordination Chemistry
ISSN 0095-8972 print/ISSN 1029-0389 online © 2009 Taylor & Francis
DOI: 10.1080/00958970903159149

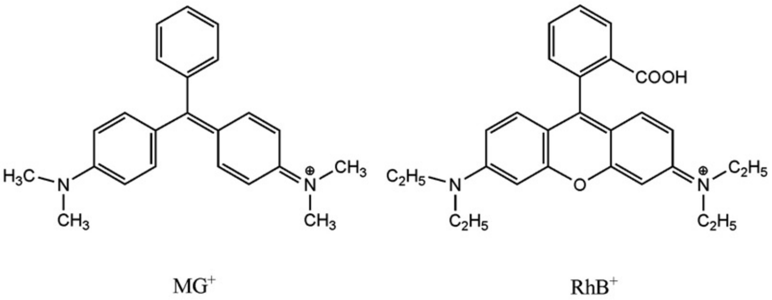
Scheme 1. The molecular structures of cations in **1** and **2**.

quasi-1-D spin system through controlling assembly of the paramagnetic $[M(mnt)_2]^-$ architectures. In previous studies, benzylpyridinium derivatives, as counter cations, were chosen to tune the stack structure of $[Ni(mnt)_2]^-$ architectures, and a series of quasi-1-D spin systems were obtained, some of which exhibit novel spin-Peierls-like transition [10–13].

The $[Ni(dmit)_2]^-$ (where $dmit^{2-} = $ 1,3-dithiole-2-thione-4,5-dithiolate) is the analog of $[Ni(mnt)_2]^-$ (both anions possess planar geometry and delocalized electronic structure with $S = ½$), and is also an excellent building block for molecular magnetic materials in addition to well-known electric conductivity [14–19]. In comparison with $[Ni(mnt)_2]^-$, there exist multiple intermolecular $S \cdots S$ contacts in $[Ni(dmit)_2]^-$, for example, head-to-head and lateral-to-lateral $S \cdots S$ contacts between $[Ni(dmit)_2]^-$ anions besides face-to-face $S \cdots S$ stacks observed in $[Ni(mnt)_2]^-$. The multiple intermolecular $S \cdots S$ interactions could give diverse stacking structures of $[Ni(dmit)_2]^-$ anions, such as 1-D ladder or 2-D layer structures, which could exhibit different physical properties.

In this article, we report the structures and magnetic properties for two complexes, $[MG][Ni(dmit)_2]$ (**1**) and $[RhB][Ni(dmit)_2]$ (**2**) ($MG^+ = $ N-(4-((4-(dimethylamino) phenyl)(phenyl)methylene)cyclohexa-2,5-dienylidene)-N-methylmethanaminium; $RhB^+ = $ 9-(2-carboxyphenyl)-3,6-bis(diethylamino)xanthylium (scheme 1).

2. Experimental

2.1. *Chemicals and reagents*

All reagents and chemicals were purchased from commercial sources and used without purification. The $(Bu_4N)[Ni(dmit)_2]$ was synthesized following the literature procedures [20, 21].

2.2. *Physical measurements*

Elemental analyses were performed with an Elementar Vario EL III analytic instrument. IR spectra were recorded on a Bruker Vector 22 Fourier transform infrared spectrometer (170SX) (KBr disc). Magnetic susceptibility data on polycrystalline samples were collected over the temperature range 2–350 K using a Quantum Design MPMS-XL superconducting quantum interference device (SQUID) magnetometer.

2.3. *Preparations for 1 and 2*

2.3.1. (MG)[Ni(dmit)$_2$] (1).

A MeCN solution (10 cm^3) of malachite green (48 mg, 0.1 mmol) was slowly added to a MeCN solution (20 cm^3) of (Bu$_4$N)[Ni(dmit)$_2$] (69 mg, 0.1 mmol) stirring for 15 min, then the mixture was allowed to stand overnight, and black microcrystals were filtered off, washed with MeOH, and dried under vacuum at 80°C. Yield: ~81%. Anal. Calcd for $C_{29}H_{25}N_2NiS_{10}$: C, 44.61; H, 3.23; N, 3.59; Found: C, 44.89; H, 3.48; N, 3.53%. IR spectrum (KBr disc, cm^{-1}): 2922w assigned to $\nu_{(C\text{–}H)}$ of $-CH_3$; 1612 and 1580 m contributed from $\nu_{(C=C)}$ of benzene ring; 1350 and 1055 m assigned to $\nu_{(C=C)}$, $\nu_{(C=S)}$ of dmit^{2-}.

2.3.2. (RB)[Ni(dmit)$_2$] (2).

This complex was obtained from the procedure described for **1**, but malachite green was replaced with rhodamine B as the starting material. Yield: ~74%. Anal. Calcd for $C_{34}H_{31}N_2NiO_3S_{10}$: C, 45.63; H, 3.49; N, 3.13; Found: C, 45.69; H, 3.53; N, 3.05%. IR spectrum (KBr disc, cm^{-1}): 2968 w, 2926 w assigned to $\nu_{(C\text{–}H)}$ of $-CH_3$ and $-CH_2-$; 1686 m from $\nu_{(C=O)}$ of $-COOH$; 1646, 1586 and 1553 m contributed from $\nu_{(C=C)}$ of benzene ring; 1349 and 1058 m assigned to $\nu_{(C=C)}$, $\nu_{(C=S)}$ of dmit^{2-}, respectively.

The single crystals with black-block shape suitable for X-ray analysis for **1** and **2** were obtained via recrystallizing the complexes in CH_2Cl_2.

2.4. *X-ray crystallography*

Crystallographic data for **1** (at 150 K) and **2** (at 296 and 150 K) were collected using a Bruker SMART APEX CCD-based diffractometer with graphite-monochromated Mo-Kα radiation ($\lambda = 0.71073$ Å). Data reductions and absorption corrections were performed with SAINT and SADABS software packages [22], respectively. Structures were solved by direct methods using SHELXL-97 [23]. The nonhydrogen atoms were refined anisotropically using full-matrix least-squares on F^2. All hydrogens were placed at calculated positions (C–H = 0.930 Å for benzene, 0.960 Å for methyl, 0.970 for methylene, and 0.820 Å for –OH) and refined riding on the parent atoms with $U(\mathrm{H}) = 1.2\,U_{\mathrm{eq}}$ (bonded C of both benzene and methyl group or O atoms) and $U(\mathrm{H}) = 1.5\,U_{\mathrm{eq}}$ (bonded C of methyl group). For **1**, the asymmetric unit contains one half of a CH_2Cl_2, in which carbon coincides with an inversion center, chloride disordered with four positions and hydrogens of CH_2Cl_2 not added. For **2**, two ethyl groups at 296 K and one ethyl group at 150 K in the cation are disordered over two positions; the occupancy factors for each disordered part were refined. Crystals for **1** and **2** have good appearance; however, the parameters R_{int} and R_{sigma} as well as R factors are rather high. Details of the crystallographic parameters, data collection, and refinements for **1** at 150 K and **2** at 296 and 150 K are summarized in table 1.

Table 1. Crystallographic and refinement data for **1** and **2**.

Complex	**1** · $0.5CH_2Cl_2$	**2** (296 K)	**2** (150 K)
Empirical formula	$C_{29}H_{25}N_2NiS_{10} \cdot 0.5CH_2Cl_2$	$C_{34}H_{31}N_2NiO_3S_{10}$	$C_{34}H_{31}N_2NiO_3S_{10}$
Formula weight	823.28	894.92	894.92
Wavelength (Å)	0.71073	0.71073	0.71073
Space group	$P2_1/c$	$P\text{-}1$	$P\text{-}1$
Temperature (K)	150(2)	296(2)	150(2)
Unit cell dimensions (Å, °)			
a	19.374(5)	10.419(5)	10.2609(10)
b	12.343(3)	10.960(6)	10.8122(12)
c	14.698(4)	18.320(9)	18.3869(15)
α	90.000	105.333(8)	105.596(7)
β	95.773(10)	96.999(7)	96.330(7)
γ	90.000	90.659(7)	91.293(7)
Volume (Å^3), Z	3497.0(16), 4	2000.3(17), 2	1949.9(3), 2
Calculated density (g cm^{-3})	1.564	1.486	1.524
Absorption coefficient (mm^{-1})	1.254	1.044	1.071
R_1	0.0765	0.0490	0.0609
wR_2	0.1945	0.1000	0.1118

$R_1 = \Sigma\|F_o| - |F_c\|/\Sigma|F_o|$ and $wR_2 = \{\Sigma[w(F_o{}^2 - F_c{}^2)^2]/\Sigma[w(F_o{}^2)^2]\}^{1/2}$.

3. Results and discussion

3.1. *Crystal structure of 1*

Complex **1** crystallizes in the monoclinic space group $P2_1/c$ with one $[Ni(dmit)_2]^-$ and one MG^+ together with one half of disordered CH_2Cl_2 in an asymmetric unit. The molecular structures of anion and cation are shown in figure 1(a), and selected bond lengths and angles with their estimated standard deviations for the anion of **1** are listed in table S1. The anion shows a banana shape molecular structure (illustrated in figure 1b), the square-planar NiS_4 coordination core makes dihedral angles of 4.47 and 7.63° with the mean molecular planes of two $dmit^{2-}$ ligands. The bond lengths and angles are comparable to reported $[Ni(dmit)_2]^-$ complexes [16–19]. The cation of MG^+ possesses a three-blade propeller shape; for the sake of convenience, three blades are, respectively, labeled as A, B (two N,N′-dimethylaminophenyl groups; where A and B contain C10-atom and C16-atom, respectively) and C (the phenyl group), the dihedral angle is 39.25° between the benzene rings of A and B moieties; 64.55° between the benzene rings of A and C; and 60.62° between the benzene rings of B and C. Six CC bond lengths in the benzene ring are quite close to each other in the range 1.376(15)–1.397(13) Å for C moiety, while exhibiting alternating C–C and C=C characteristics for both A and B (figure S1). Delocalization of the positive charge leads to C11–N1 (1.361(11) Å) and C19–N2 (1.328(10) Å) showing considerable double bond character.

As illustrated in figure 2, the two neighboring anions form a lateral-to-lateral dimer with shorter interatomic separations, 3.5783(35) Å of $S(7) \cdots S(5)^i$, 3.5527(34) Å of $S(7) \cdots S(6)^i$ (symmetric code $i = 1-x, 1-y, -z$). Adjacent $[Ni(dmit)_2]^-$ dimers link into 1-D chains along crystallographic [1 1 0] direction through intermolecular head-to-head S ··· S interactions with $S(3) \cdots S(3)^{ii} = 3.4839(64)$ Å (symmetric code $ii = -x, -y, -z$).

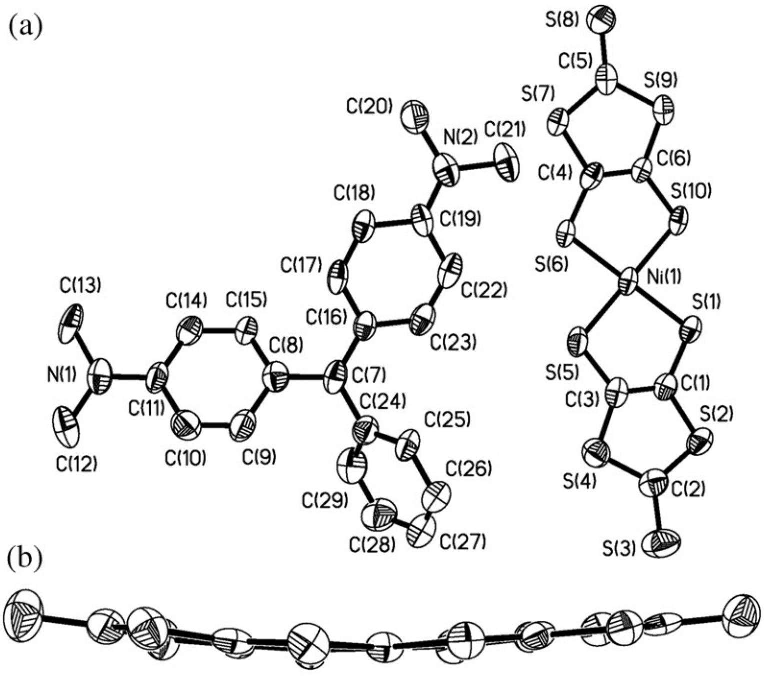

Figure 1. (a) ORTEP view of **1** with thermal ellipsoids at the 50% probability level. (b) The side view of anion shows the banana shape.

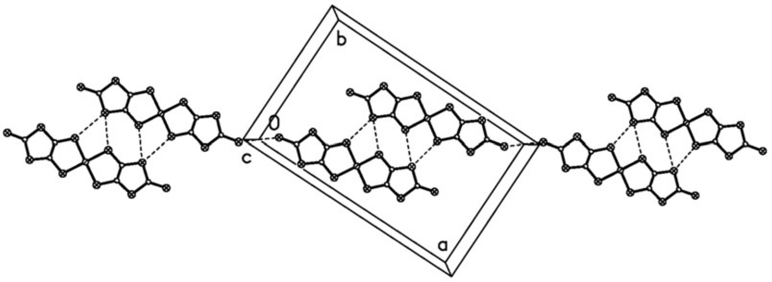

Figure 2. The adjacent anionic dimers link into 1-D chain via head-to-head S···S contact along crystallographic [1 1 0] direction in the crystal of **1**.

3.2. *Crystal structure of 2 at 296 and 150 K*

The crystal structure of **2** at 100 K was reported by Soneta *et al.* [24], which showed one ethyl of the cation disordered. In the low-dimensional (1-D or 2-D) spin system, there exists strong spin-lattice interaction [25–28]. As a consequence, the structural disorder-to-order change probably induces a change of magnetic property [29]. This is our motivation to check the crystal structures at room- and low-temperature for this complex again. Complex **2** crystallizes in the triclinic space group *P*-1 at 296 K, its

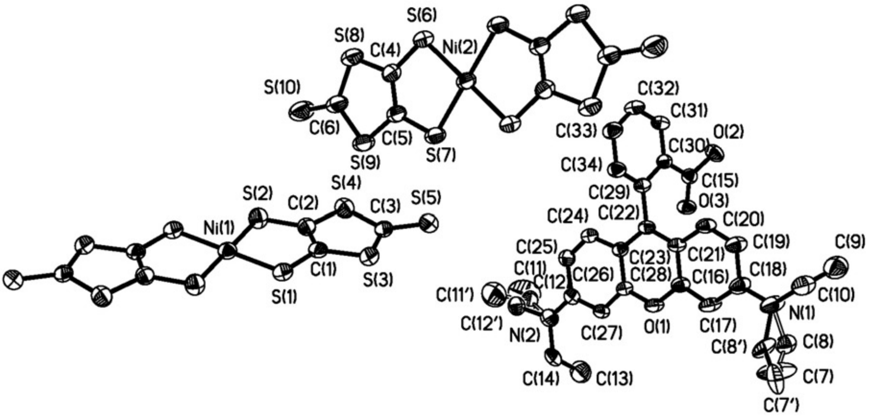

Figure 3. ORTEP view for **2** with non-hydrogen atomic labeling and the thermal ellipsoids at 30% probability level.

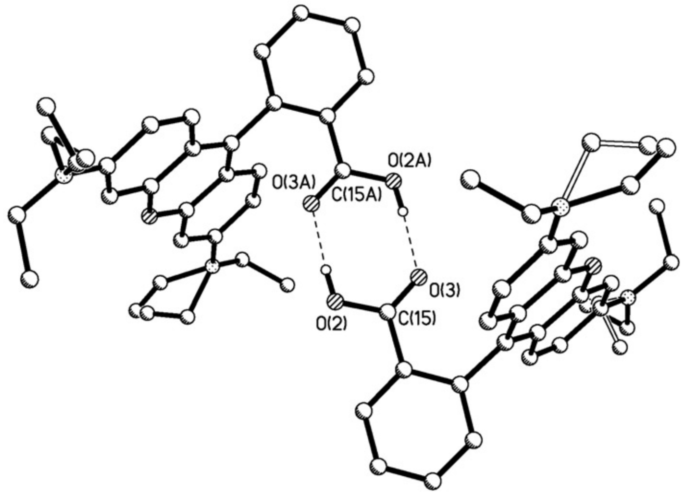

Figure 4. Complementary hydrogen-bond pair between carboxyl groups of cations in the crystal of **2**.

asymmetric unit composed of two half anions together with one cation; the Ni-ions in two inequivalent anions locate on an inversion center as shown in figure 3. Two crystallographically independent anions exhibit perfect planar geometry with the two mean molecular planes making a dihedral angle of 68.65°. Bond lengths and angles are comparable to those in **1** (table S1), and also in good agreement with various $[Ni(dmit)_2]^-$ complexes [16–19]. For the cation, the xanthene moiety is planar (figure 3), and the mean molecular plane of xanthene makes a dihedral angle of 75.35° with the mean plane of phenyl. Delocalization of the positive charge between the nitrogen and the benzene ring is evidenced by C18–N1 and C26–N2 bonds of 1.337(5) and 1.353(5) Å, respectively, showing significant double bond character. Two of the four ethyl groups exhibit serious disorder. Figure 4 displays a rigid cationic dimer which

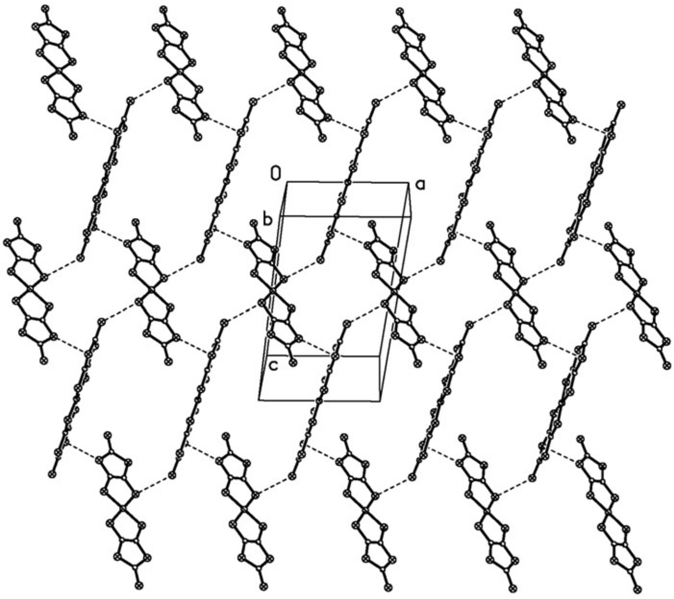

Figure 5. Anions forming a molecular sheet via intermolecular lateral-to-lateral and head-to-lateral S ⋯ S interactions in **2**; the sheet is parallel to the crystallographic plane (0 1 −1).

forms via strong complementary hydrogen-bond pairs between carboxyl groups with the geometric parameters of $\angle$O2–H2A ⋯ O3A = 177.37 and $d_{O3A \cdots O2} = 2.661(3)$ Å (symmetric code: A = $-x$, $1-y$, $2-z$). Neighboring cationic dimers arrange into a layer which is parallel to the crystallographic (0 1 −1) plane. Adjacent anions form a molecular sheet via lateral-to-lateral and lateral-to-head intermolecular S ⋯ S interactions with shorter interatomic contacts, $d_{S4 \cdots S9} = 3.582(18)$ Å and $d_{S5 \cdots S6A} = 3.681(19)$ Å (symmetric code: A = $x-1$, y, z). The anionic sheet is also parallel to the crystallographic (0 1 −1) plane (figure 5). The anionic (A) and cationic (C) layers arrange in the alternating manner of ⋯ ACACAC ⋯ in the solid state.

The structure of **2** at 150 K is similar to that at 296 K, and the intramolecular geometric parameters in both anions and cations at 150 K are quite close to those at 296 K. Comparing the structures at 296 and 150 K, the main differences are: (1) upon cooling the *a*- and *b*-axes shrink while *c* increases; (2) two ethyl groups are disordered at 296 K while only one at 150 K; and (3) enhanced intermolecular S ⋯ S interactions are observed at 150 K (the interatomic contacts of $d_{S4 \cdots S9} = 3.526(15)$ Å and $d_{S5 \cdots S6A} = 3.571(16)$ Å (symmetric code: A = $x-1$, y, z).

3.3. *Magnetic susceptibilities of 1 and 2*

Variable-temperature magnetic properties of **1** and **2** have been investigated in the temperature range 2–350 K. The plots of magnetic susceptibility are displayed in the forms of $\chi_m = f(T)$ in figure 6. From the crystal structure, paramagnetic anions form 1-D alternating chains in **1**, but the temperature dependence of magnetic susceptibility does not show the magnetic character of a 1-D spin system; magnetic susceptibility data

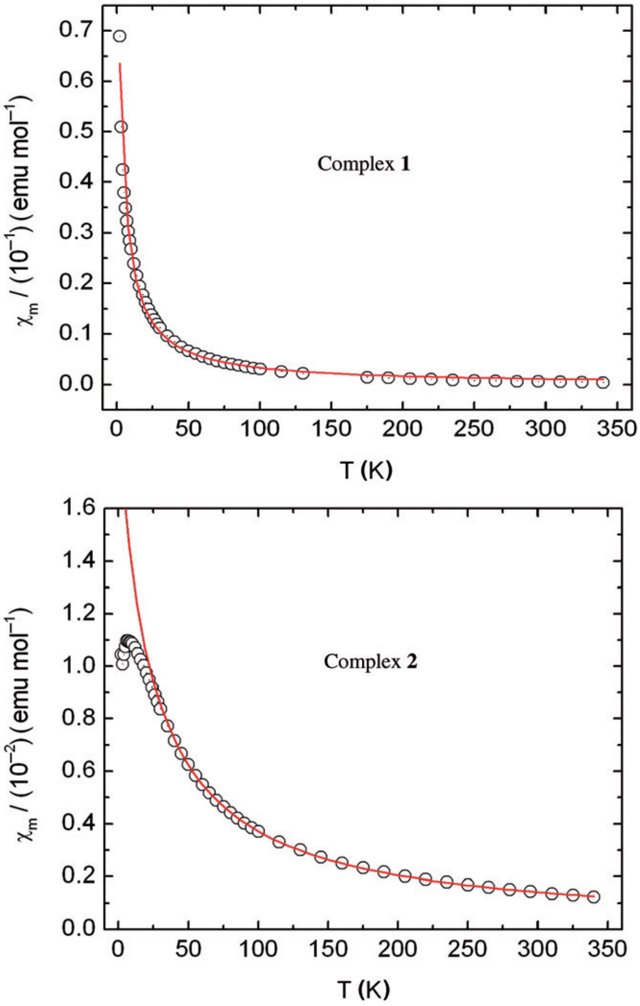

Figure 6. Temperature dependences of magnetic susceptibility in χ_m form for **1** and **2** (○ experimental data, (—) solid lines: reproduced from the fitting parameters).

with simple Curie–Weiss behavior were fit to equation (1) with Curie constant $C = 0.351(15)\,\mathrm{emu\,K\,mol^{-1}}$, Weiss constant $\theta = -3.51(28)\,\mathrm{K}$, and the contributions from the core diamagnetism and possible van Vleck paramagnetism $\chi_0 = 8.00(3) \times 10^{-5}\,\mathrm{emu\,mol^{-1}}$.

$$\chi_m = C/(T - \theta) + \chi_0. \tag{1}$$

The plot χ_m *versus* T of **2** exhibits a maximum around 6 K which corresponds to the 1-D or 2-D antiferromagnetic Heisenberg model. From the crystal structure, the 2-D magnetic exchange model may be reasonable. Magnetic susceptibility in the temperature range 45–350 K was fit to equation (1) to give $C = 0.463(3)\,\mathrm{emu\,K\,mol^{-1}}$, $\theta = -24.1(4)\,\mathrm{K}$ and $\chi_0 = 2(1) \times 10^{-5}\,\mathrm{emu\,mol^{-1}}$. The crystal structures at 296 and 150 K disclosed disordered-to-ordered transition occurs for one ethyl of the cation, but no change of magnetic property in the temperature range 150–296 K reveals the magnetoelastic coupling interaction in this spin system is weak.

4. Conclusions

Crystal structures and magnetic properties for two complexes of $[Ni(dmit)_2]^-$ with dye cations have been investigated. For **1**, the paramagnetic $[Ni(dmit)_2]^-$ anions form a 1-D dimerized chain via intermolecular $S \cdots S$ contacts, whereas the temperature dependence of magnetic susceptibility shows a simple Curie–Weiss behavior with weak antiferromagnetic coupling interactions between neighboring magnetic centers. In **2**, the paramagnetic $[Ni(dmit)_2]^-$ anions construct 2-D molecular layers via intermolecular $S \cdots S$ contacts. Weak antiferromagnetic coupling interactions dominate within the anionic layers, and this 2-D spin system possesses weak magnetoelastic coupling.

Supplementary material

CCDC 727558, 716166, and 727557 contain the supplementary crystallographic data of **1**, **2** (296K), and **2** (150K). These data can be obtained free of charge from the Cambridge Crystallographic Data Center via http://www.ccdc.cam.ac.uk/data_request/cif

Acknowledgments

The authors thank the Science and Technology Department of Jiangsu Province and NSFC of China for financial support (Grant Nos: BK2007184, 20871068, and 10774076). X. M. Ren thanks Professor Akutagawa for the magnetic susceptibility measurements.

References

[1] F. Bigoli, P. Deplano, F.A. Devillanova, V. Lippolis, P.J. Lukes, M.L. Mercuri, M.A. Pellinghelli, E.F. Trogu. *J. Chem. Soc., Chem. Commun.*, 371 (1995).

[2] U.T. Mueller-Westerhoff, B. Vance, D.I. Yoon. *Tetrahedron*, **47**, 909 (1991).

[3] H. Tanaka, H. Kobayashi, A. Kobayashi. *J. Am. Chem. Soc.*, **124**, 10002 (2002).

[4] H. Tanaka, Y. Okano, H. Kobayashi, W. Suzuki, A. Kobayashi. *Science*, **291**, 285 (2001).

[5] T. Akutagawa, H. Koshinaka, D. Sato, S. Takeda, S.-I. Noro, H. Takahashi, R. Kumai, Y. Tokura, T. Nakamura1. *Nature Mater.*, **8**, 342 (2009).

[6] A.T. Coomber, D. Beljonne, R.H. Friend, J.K. Bredas, A. Charlton, N. Robertson, A.E. Underhill, M. Kurmoo, P. Day. *Nature*, **380**, 144 (1996).

[7] N. Robertson, L. Cronin. *Coord. Chem. Rev.*, **227**, 93 (2002).

[8] F. Bigoli, C.T. Chen, W.C. Wu, P. Deplano, M.L. Mercuri, M.A. Pellinghelli, L. Pilia, G. Pintus, A. Serpe, E.F. Trogu. *Chem. Commun.*, 2246 (2001).

[9] C.S. Winter, C.A.S. Hill, A.E. Underhill. *Appl. Phys. Lett.*, **58**, 107 (1991).

[10] X.M. Ren, Q.J. Meng, Y. Song, C.S. Lu, C.J. Hu. *Inorg. Chem.*, **41**, 5686 (2002).
[11] X.M. Ren, S. Nishihara, T. Akutagawa, S. Noro, T. Nakamura. *Inorg. Chem.*, **45**, 2229 (2006).
[12] Z.F. Tian, X.M. Ren, Y.Z. Li, Y. Song, Q.J. Meng. *Inorg. Chem.*, **46**, 8102 (2007).
[13] D.B. Dang, C.L. Ni, Y. Bai, Z.F. Tian, Z.P. Ni, L.L. Wen, Q.J. Meng, S. Gao. *Chem. Lett.*, **5**, 680 (2005).
[14] P.I. Clemenson. *Coord. Chem. Rev.*, **106**, 171 (1990).
[15] T. Akutagawa, T. Nakamura. *Coord. Chem. Rev.*, **226**, 3 (2002).
[16] T. Akutagawa, T. Nakamura. *Coord. Chem. Rev.*, **198**, 297 (2000).
[17] T. Akutagawa, K. Shitagami, S. Nishihara, S. Takeda, T. Hasegawa, T. Nakamura, Y. Hosokoshi, K. Inoue, S. Ikeuchi, Y. Miyazaki, K. Saito. *J. Am. Chem. Soc.*, **127**, 4397 (2005).
[18] S. Nishihara, T. Akutagawa, T. Hasegawa, T. Nakamura. *Chem. Commun.*, 408 (2002).
[19] T. Akutagawa, T. Hasegawa, T. Nakamura, S. Takeda, T. Inabe, K. Sugiura, Y. Sakata, A.E. Underhill. *Chem. Eur. J.*, **7**, 4902 (2007).
[20] G. Steimecke, H.J. Sieler, R. Kirmse, E. Hoyer. *Phosphorus Sulfur*, **7**, 49 (1979).
[21] W.J. Tong, L. Liu, Q.J. Meng, Y.Z. Li. *Acta Cryst.*, **E58**, m724 (2002).
[22] *Software Packages SMART and SAINT*, Siemens Analytical X-ray Instrument Inc., Madison, WI (1996).
[23] G.M. Sheldrick. *SHELXL*-97, *Program for the Refinement of Crystal Structure*, University of Göttingen, Germany (1997).
[24] Y. Soneta, S. Sakamoto, K. Miyamura. *Acta Cryst.*, **E62**, m3448 (2006).
[25] R.E. Peierls. *Quantum Theory of Solids*, p. 108, Oxford University Press, London, England (1955).
[26] J.W. Bray, H.R. Hart, L.V. Interrante Jr., L.S. Jacobs, J.S. Kasper, G.D. Watkins, S.H. Wee. *Phys. Rev. Lett.*, **35**, 744 (1975).
[27] R.K. Kremer, I. Loa, F.S. Razavi, K. Syassen. *Solid State Commun.*, **113**, 217 (2000).
[28] X.M. Ren, S. Nishihara, T. Akutagawa, S. Noro, T. Nakamura, W. Fujita, K. Awaga. *Chem. Phys. Lett.*, **439**, 318 (2007).
[29] O. Jeannin, R. Clérac, M. Fourmigué. *J. Am. Chem. Soc.*, **128**, 14649 (2006).